Mechanics Based Design of Structures and Machines: An International Journal
Publication details, including instructions for authors and subscription information:
http://www.tandfonline.com/loi/lmbd20

Static Damage Identification of 3D and 2D Frames

M. Rezaiee-Pajand [a], M. S. Kazemiyan [a] & A. Aftabi. S [b]
[a] Department of Civil Engineering, Ferdowsi University of Mashhad, Iran
[b] Department of Civil Engineering, Islamic Azad University of Mashhad, Iran
Accepted author version posted online: 08 Aug 2013.Published online: 04 Dec 2013.

To cite this article: M. Rezaiee-Pajand, M. S. Kazemiyan & A. Aftabi. S (2014) Static Damage Identification of 3D and 2D Frames, Mechanics Based Design of Structures and Machines: An International Journal, 42:1, 70-96, DOI: 10.1080/15397734.2013.830534

To link to this article: http://dx.doi.org/10.1080/15397734.2013.830534

Mechanics Based Design of Structures and Machines, 42: 70–96, 2014

ISSN: 1539-7734 print/1539-7742 online
DOI: 10.1080/15397734.2013.830534

STATIC DAMAGE IDENTIFICATION OF 3D AND 2D FRAMES#

M. Rezaiee-Pajand[1], M. S. Kazemiyan[1], and A. Aftabi. S[2]
[1]*Department of Civil Engineering, Ferdowsi University of Mashhad, Iran*
[2]*Department of Civil Engineering, Islamic Azad University of Mashhad, Iran*

A new algorithm for static damage detection of three- and two-dimensional frames is presented in this paper. This approach is based on the minimization of difference between the measured and analytical static displacements of frames. The damage detection problem is solved as a nonlinear constrained structural optimization. In this strategy, the global structural stiffness matrix is parameterized. To achieve the goal, a new technique based on the eigen decomposition of the local elemental stiffness matrix is suggested. Structural damage is modeled as a reduction in cross-sectional properties of the elements. It is assumed that the stiffness matrix of the structure is perturbed due to damage. Hence, the damaged structural stiffness matrix is presumed to be the sum of the stiffness matrix of the undamaged structure and the perturbation matrix. Consequently, the sum of these matrices should be inverted in each iteration. Instead of the common ways of inversion, Sherman–Morrison–Woodbury formula is employed. Prior to the outset of the optimization procedure, the number of design variables, the amount of reductions in cross-sectional properties, is decreased by introducing a new suggested technique. This scheme is based on the nodal equilibrium equations. To illustrate the robustness and efficiency of the authors' algorithm, several numerical problems are solved.

Keywords: Damage assessment; Frame structure; Matrix inversion; Optimization; Static problem; Sherman–Morrison–Woodbury formula; Updated matrix.

1. INTRODUCTION

Recently, damage detection of structures has received considerable attention from various fields of engineering, such as civil, mechanical, and aerospace engineering. As a result, the extensive researches have been conducted in this field, and large amounts of techniques for damage identification of structures have been proposed. These strategies are classified into two categories: (1) static methods and (2) dynamic methods. The former utilizes the static responses of structures, such as displacements and strains, to locate and estimate the severity of damage in structures. On the other hand, the latter uses the dynamic characteristics, such as frequencies and shape modes, to detect damage in structures. Both groups are usually based on finite element analysis and the results of experiments. The main

Received November 1, 2012; Accepted July 5, 2013
#Communicated by I. Elishakoff.
Correspondence: M. Rezaiee-Pajand, Professor, Department of Civil Engineering, Ferdowsi University of Mashhad, P.O. Box. 91775-1111, Iran; E-mail: mrpajand@yahoo.com

idea of these approaches is that the mass, damping, and stiffness properties of the structures alter after the occurrence of damage. Consequently, the static and dynamic responses of the structures change. These processes aim to adapt the finite element model to match the analytical and the measured responses. In this way, these algorithms detect the magnitude and the location of damage in structures.

Compared with the static approaches, dynamic ones are more complicated because changes in dynamic responses are rooted in alteration of mass, damping, and stiffness properties, whereas change in static responses is only involved in stiffness properties. To remedy this difficulty, most of the dynamic schemes ignore damping and variation of mass. Moreover, the static tests are more accurate than the dynamic ones because the high orders of modal data are required to identify damages through the stiffness properties, and it is really difficult to obtain these data. Furthermore, it is challenging to achieve the accurate mode shapes on some stiff structures. In addition, static tests are cheaper than the dynamic ones. For all these reasons, static methods have drawn considerable attention in recent years.

Dynamic approaches have developed more fully than the static ones. Ramamurti and Neogy (1998) proposed a tactic to detect damage in blades of turbo machines. In this technique, the natural frequency is considered as a damage criterion. Akgun and Ju (1990) investigate the effects of cracks in planar frames. Then, they proposed a dynamic method to determine the location and severity of cracks. In some damage identification approaches, structural analysis must be performed repeatedly to detect the worst damage scenario. Aktas and Moses (1998) approximated the dynamic reanalysis of unhealthy structures by using binomial series approximation. Some researchers have provided an exhaustive literature review on the work in this area (Carden and Fanning, 2004). This survey investigates the characteristics and the formulations of various dynamic approaches. Compared with the dynamic methods, the literature on the static techniques is few. The following paragraph is devoted to briefly summarize the state of the art of the static damage detection techniques. Sheena et al. (1982) endeavored to minimize the discrepancies between the actual and analytical stiffness matrix by updating the elements of the stiffness matrix. They utilized noise-free measurements in their strategy. Sanayei and Nelson (1986) introduce a scheme in which displacements were measured to calculate the structural stiffness properties. In their algorithm, the applied force degrees of freedom (DOFs) and the measured ones had to be totally overlapped; therefore, this tactic was not practical. Sanayei and Onipede (1991) removed the disadvantage of Sanayei and Nelson (1986). Their way did not require the external loads to be applied at the measured DOFs. Sanayei and Saletnik (1996a, Part I) locate and estimate the severity of damage in structures by measuring some of the elemental strains. They also investigated the effect of noisy data on their methods (Sanayei and Saletnik, 1996b, Part II). Hajela and Soeiro (1990a,b) classified the existing parameter identification tactics into three groups: (1) equation error (2) output error (3) minimum deviation techniques. Besides, they identify damage in structures by utilizing both dynamic and static responses. Banan et al. (1994a, Part I, 1994b, Part II) presented two algorithms to detect the location and the magnitude of damage in structures. These researchers employed Recursive Quadratic programming method for solving the optimization problem. Hjelmstad and Shin (1997) proposed a scheme to detect damage by measuring the static responses. It should be noted that this process is based on

the research conducted by Banan et al. (1994a, Part I, 1994b, Part II) and Liu and Chian (1997) obtained a new shape of the equilibrium equation of trusses. In this way, the parameters of the stiffness matrix were separated from other elements of this matrix. They also detected damage in trusses by utilizing their new formulation. Rezaiee-Pajand and Saliani (2004) developed the suggested approach by Liu and Chian (1997). Their tactic was capable of identifying damage in trusses by measuring displacements. Besides, they compared the robustness of several existing damage detection methods. Chou and Ghaboussi (2001) used genetic algorithm to assess damage in structures. Bakhtiari-Nejad et al. (2005) proposed a technique for static damage detection of structures. In addition, they formulate the problem as a nonlinear optimization problem solved by Sequential Quadratic programming (SQP). Shenton III and Hu (2006) detected damage in structures by utilizing dead load redistribution. Kouchmeshky et al. (2007) studied the problem of damage detection using minimum test data. Rezaiee-Pajand and Aftabi Sani (2008) presented a strategy to locate damage and estimate its severity. Their formulation led to a Binary programming solved by pseudo-dual simplex procedure. Yang and Sun (2010) applied the flexibility disassembly technique to identify the location and the extent of damage in structures. Note that they identified structural damage without using the optimization methods. Abdo (2012) investigated the relationship between the locations and severity of damage with the displacement curvature of beams. In addition to the above-cited damage identification methods, some researchers have proposed closed-form solutions for damage identification of structures. For example, Caddemi et al. have presented accurate closed-form expressions for detecting the location and severity of cracks in elastic beams (Caddemi and Greco, 2006; Caddemi and Morassi, 2007, 2011). Dong et al. (2002) have demonstrated that utilizing local parameters can be more effective to detect damage in structures, in comparison with the global ones. One of the key parameters in some failure criteria of ductile material is the damage related to the voids. Alves (2001) modeled this type of damage as changes in Young's modulus.

In this study, a new method to locate and estimate the magnitude of damage in 3D and 2D frames is proposed. This technique utilizes the structural displacements. The overall formulation leads to a nonlinear optimization problem, in which the discrepancies between the analytical and measured displacements are minimized. In this algorithm, the damage is modeled as a reduction in cross-sectional properties, which perturbs the stiffness matrix of the healthy structure. Consequently, the damaged stiffness matrix is assumed to be the sum of the stiffness matrix of the undamaged structure and the perturbation matrix. To establish the goal function, the sum of the aforementioned matrices must be inverted. To efficiently and accurately calculate the inversion of the sum of two matrices, Sherman–Morrison–Woodbury formula is employed. Previously, this formula has not been utilized for the construction of the objective function, which is used in damage detection problems. Some researchers have applied second-order Taylor's series to set up this goal function (Bakhtiari-Nejad et al., 2005). It is worth emphasizing; the latter formulation is approximate and produces some numerical errors. It should be added that the suggested approach models the damage, which is represented by a reduction of the cross-sectional properties of an entire element. Consequently, the proposed approach cannot localize concentrated damage within the element length. Moreover, the number of design variables is reduced by introducing a new technique based

on nodal equilibrium equations. Finally, several numerical tests are performed to demonstrate the capability and efficiency of the suggested method.

2. PARAMETERIZATION OF THE STIFFNESS MATRIX

As previously mentioned, the unknown parameters of the damage detection problem are the cross-sectional properties of the damaged structures. The damage identification algorithms aim to estimate these parameters. To formulate the authors' damage assessment technique, it is essential to parameterize the global stiffness matrix. To achieve this goal, a new method based on the eigen decomposition of elements' local stiffness matrices is presented. Herein, this approach is comprehensively demonstrated for 2D beam element without axial DOF, and the related results for 2D and 3D frame elements are solely mentioned in Appendix A.

Consider the 2D beam element in Fig. 1. As it is shown in this figure, the beam element has both rotational and translational DOFs, which results in the unusual mixed units of length and radians in the eigenvalues and eigenvectors of the local stiffness matrix (Doebling et al., 1998). This inconsistency is rooted in the well-known shape functions of the element.

The shape functions of this element are as below (Rezaiee-Pajand and Moayyedian, 2004):

$$\begin{aligned} N_1(x) &= 1 - \frac{3x^2}{L^2} + \frac{2x^3}{L^3}, \\ N_2(x) &= x - \frac{2x^2}{L} + \frac{x^3}{L^2}, \\ N_3(x) &= \frac{3x^2}{L^2} - \frac{2x^3}{L^3}, \\ N_4(x) &= \frac{x^3}{L^2} - \frac{x^2}{L}, \end{aligned} \tag{1}$$

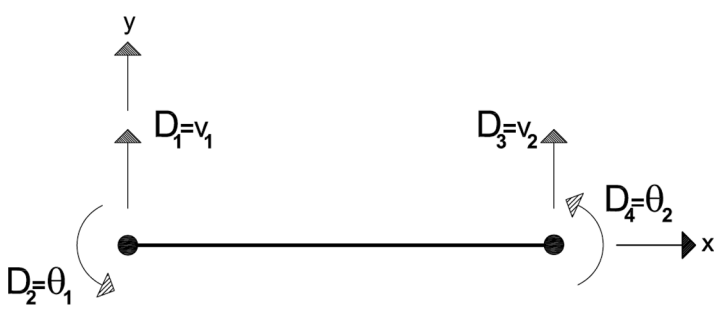

Figure 1 2D beam element.

where the length of the element is L. By employing the aforementioned shape functions, the displacement function can be computed as follows:

$$v(x) = N_1(x)\, v_1 + N_2(x)\, \theta_1 + N_3(x)\, v_2 + N_4(x)\, \theta_2. \tag{2}$$

Alternatively, in matrix notation, the succeeding relationship is held:

$$v(x) = [N_1(x) \quad N_2(x) \quad N_3(x) \quad N_4(x)] \begin{Bmatrix} D_1 \\ D_2 \\ D_3 \\ D_4 \end{Bmatrix} = \mathbf{N}\,\mathbf{D}_E. \tag{3}$$

In the last relation, $\mathbf{N}$ denotes the row matrix of the shape functions, and the elemental displacement vector is $\mathbf{D}_E$. To calculate the local stiffness matrix, the next equality is usually deployed (Rezaiee-Pajand and Moayyedian, 2004):

$$\mathbf{K}_E = \int_0^L \mathbf{B}^T (EI_z)\mathbf{B}\, dx \tag{4}$$

in which

$$\mathbf{B} = [N_1''(x) \quad N_2''(x) \quad N_3''(x) \quad N_4''(x)]. \tag{5}$$

In Eq. (4), I_z is the beam moment of inertia with respect to the z axis, E is the Young's modulus. Moreover, the $\mathbf{B}$ matrix contains the second-order derivatives of shape functions. By using these shape functions, the local stiffness matrix is obtained in the subsequent form:

$$\mathbf{K}_E = \frac{EI_z}{L^3} \begin{bmatrix} 12 & 6L & -12 & 6L \\ 6L & 4L^2 & -6L & 2L^2 \\ -12 & -6L & 12 & -6L \\ 6L & 2L^2 & -6L & 4L^2 \end{bmatrix}. \tag{6}$$

Clearly, since the beam element has both translational and rotational DOFs, the units of the shape functions and the entries of $\mathbf{K}_E$ are inconsistent. In addition, if eigen-decomposition is employed for $\mathbf{K}_E$, this inconsistency will lead to appearance of mixed units in the eigenvalues and eigenvectors as well.

The inconsistency of units of the element stiffness matrix was avoided by some other researchers (Caddemi and Calio, 2013; Calio and Greco, 2013). They multiplied the rotations and the forces by the beam length to obtain consistent units in the stiffness matrix. To cancel the mixed units, a 2D beam element with new fictitious DOFs is proposed. The suggested DOFs for the beam element have only the units of length, and as a result, all the units of these DOFs are consistent. This beam element with new virtual DOFs is demonstrated in Fig. 2.

The new shape functions of this element have the coming appearance:

$$\widehat{N}_1(x) = 1 - \frac{3x^2}{L^2} + \frac{2x^3}{L^3},$$

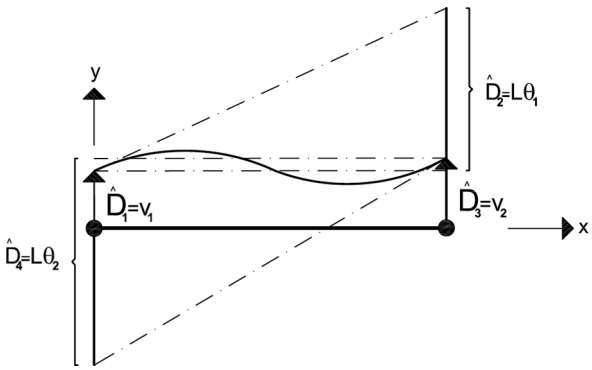

Figure 2 2D beam element with new fictitious DOFs.

$$\begin{aligned}\widehat{N}_2(x) &= \frac{x}{L} - \frac{2x^2}{L^2} + \frac{x^3}{L^3},\\ \widehat{N}_3(x) &= \frac{3x^2}{L^2} - \frac{2x^3}{L^3},\\ \widehat{N}_4(x) &= \frac{x^3}{L^3} - \frac{x^2}{L^2},\end{aligned} \tag{7}$$

Utilizing these shape functions leads to the succeeding displacement function:

$$\hat{v}(x) = \widehat{N}_1(x)\, v_1 + \widehat{N}_2(x)\,(L\theta_1) + \widehat{N}_3(x)\, v_2 + \widehat{N}_4(x)\,(L\theta_2). \tag{8}$$

This equation can be expressed in the coming matrix form:

$$\hat{v}(x) = [\widehat{N}_1(x)\ \widehat{N}_2(x)\ \widehat{N}_3(x)\ \widehat{N}_4(x)] \begin{Bmatrix} \widehat{D}_1 \\ \widehat{D}_2 \\ \widehat{D}_3 \\ \widehat{D}_4 \end{Bmatrix} = \widehat{\mathbf{N}}\,\widehat{\mathbf{D}}_E. \tag{9}$$

By comparing Eqs. (1) and (7), the following results can be obtained:

$$\mathbf{N} = \widehat{\mathbf{N}}\,\mathbf{Q}, \tag{10}$$

in which, the transformation matrix $\mathbf{Q}$ is defined as below:

$$\mathbf{Q} = \begin{bmatrix} 1 & 0 & 0 & 0 \\ 0 & L & 0 & 0 \\ 0 & 0 & 1 & 0 \\ 0 & 0 & 0 & L \end{bmatrix}. \tag{11}$$

Calculation of the second-order derivatives of $\mathbf{N}$ yields the latter matrix:

$$\mathbf{B} = \widehat{\mathbf{B}}\,\mathbf{Q}, \tag{12}$$

$$\widehat{\mathbf{B}} = [\widehat{N''}_1(x)\ \ \widehat{N''}_2(x)\ \ \widehat{N''}_3(x)\ \ \widehat{N''}_4(x)]. \tag{13}$$

It is worth emphasizing that $\mathbf{Q}$ plays a role of a constant parameter for the derivation process. Inserting Eq. (12) into Eq. (4) leads to the subsequent results:

$$\mathbf{K}_E = \int_0^L \mathbf{Q}^T \widehat{\mathbf{B}}^T EI_z \widehat{\mathbf{B}}\, \mathbf{Q}\, dx = \mathbf{Q}^T \left(\int_0^L \widehat{\mathbf{B}}^T EI_z \widehat{\mathbf{B}}\, dx \right) \mathbf{Q}, \tag{14}$$

$$\widehat{\mathbf{K}}_E = \int_0^L \widehat{\mathbf{B}}^T EI_z \widehat{\mathbf{B}}\, dx, \tag{15}$$

$$\widehat{\mathbf{K}}_E = \tfrac{EI_z}{L^3} \begin{bmatrix} 12 & 6 & -12 & 6 \\ 6 & 4 & -6 & 2 \\ -12 & -6 & 12 & -6 \\ 6 & 2 & -6 & 4 \end{bmatrix}, \tag{16}$$

$$\mathbf{K}_E = \mathbf{Q}^T \widehat{\mathbf{K}}_E\, \mathbf{Q}. \tag{17}$$

It is obvious that the mixed units have not arisen in the virtual local stiffness matrix and the shape functions of the beam element with fictitious DOFs. Consequently, the inconsistency of units does not exist in the structural element matrix. It should be added that the inconsistency of units can also be removed by normalizing the stiffness matrix. This technique was first proposed by Caddemi and Calio (2013).

At this stage, eigen decomposition can be utilized for $\mathbf{K}_E$. For this purpose, first, the eigenvalues and the eigenvectors of the new virtual element's stiffness matrix should be calculated. They are expressed as below:

$$\hat{\boldsymbol{\lambda}} = \frac{EI_z}{L^3} \begin{Bmatrix} 2 \\ 30 \end{Bmatrix}, \quad \hat{\boldsymbol{\kappa}} = \begin{bmatrix} 0 & \frac{2}{\sqrt{10}} \\ \frac{-1}{\sqrt{2}} & \frac{1}{\sqrt{10}} \\ 0 & \frac{-2}{\sqrt{10}} \\ \frac{1}{\sqrt{2}} & \frac{1}{\sqrt{10}} \end{bmatrix}. \tag{18}$$

To have the unit magnitude, the eigenvectors are normalized as follows:

$$\hat{\boldsymbol{\kappa}}\, \hat{\boldsymbol{\kappa}}^T = \mathbf{I}. \tag{19}$$

In the last equations, $\hat{\boldsymbol{\lambda}}$ is an $ng \times 1$ vector whose entries are the nonzero eigenvalues of the local stiffness matrix of the proposed element ($\widehat{\mathbf{K}}_E$). It should be added that the columns of the $\hat{\boldsymbol{\kappa}}$ are the eigenvectors of $\widehat{\mathbf{K}}_E$. Note that $\hat{\boldsymbol{\kappa}}$ does not contain the eigenvectors whose eigenvalues are zero. The latter matrix has four rows, which is equal to the number of the elemental DOFs, and two columns, which is equal to the nonzero eigenvalues. Based on the eigen decomposition, the true local stiffness matrix can be written in the following form:

$$\mathbf{K}_E = \mathbf{Q}^T \hat{\boldsymbol{\kappa}}\, \widehat{\Lambda}\, \hat{\boldsymbol{\kappa}}^T \mathbf{Q}. \tag{20}$$

In this equality, $\widehat{\boldsymbol{\Lambda}}$ is an $ng \times ng$ diagonal matrix whose diagonal entries are the eigenvalues of the element with fictitious DOFs. This expression can be further

simplified to have the following shape:

$$\mathbf{K}_E = \boldsymbol{\chi}\,\boldsymbol{\Lambda}\,\boldsymbol{\chi}T, \tag{21}$$

$$\boldsymbol{\chi} = \mathbf{Q}^T\boldsymbol{\kappa}. \tag{22}$$

Up to now, the technique of removing the inconsistency of the units for 2D beam element without axial DOF is demonstrated. At the next stage, the mentioned strategy is generalized for the 2D and 3D frame element with axial DOF. Based on finite element method, the elemental stiffness matrix of the 2D and 3D beam elements can be established by utilizing the new beam element. The eigenvalues, eigenvectors, and the transformation matrix of these elements will be presented in Appendix A.

After setting up the local stiffness matrix of the elements of the structure, the frames' stiffness matrix can be calculated by matrices assembling process. To achieve this, the transformation matrix $\boldsymbol{\Gamma}$ for each element should be defined as follows:

$$\boldsymbol{D}_{E_i} = \boldsymbol{\Gamma}_i\boldsymbol{D}. \tag{23}$$

In the last relation, the local displacement vector of the ith element and the structure's displacement vector are $\mathbf{D}_{E_i}$ and $\mathbf{D}$, respectively. $\mathbf{D}_{E_i}$ has ne entries, and $\mathbf{D}$ is an $nd \times 1$ vector. ne and nd are the number of the elemental DOFs and number of structure's DOFs, respectively. Note that $\boldsymbol{\Gamma}_i$ denotes the transformation matrix of the ith element, which relates the element's local DOFs to the global ones. By employing the transformation matrices, the global stiffness matrix can be obtained in the subsequent shape:

$$\mathbf{K} = \sum_{i=1}^{nel} \boldsymbol{\Gamma}_i^T\boldsymbol{\chi}_i\widehat{\boldsymbol{\Lambda}}_i\boldsymbol{\chi}_i^T\boldsymbol{\Gamma}_i. \tag{24}$$

This expression can be rewritten in the latter form:

$$\mathbf{K} = \mathbf{A}\widehat{\mathbf{P}}\mathbf{A}^T, \tag{25}$$

$$\mathbf{A} = [\boldsymbol{\Gamma}_1^T\boldsymbol{\chi}_1\ \boldsymbol{\Gamma}_2^T\boldsymbol{\chi}_2\ \ldots\ \boldsymbol{\Gamma}_{nel}^T\boldsymbol{\chi}_{nel}]. \tag{26}$$

In these formulas, $\widehat{\mathbf{P}}$ is a diagonal matrix, which has ($ng \times nel$) rows and ($ng \times nel$) columns. nel is the number of members. It should be noted that the diagonal entries of this matrix are the nonzero eigenvalues of the structure's elements. It is worth mentioning that the eigenvalues are related to the stiffness properties of the structure. In addition, $\mathbf{A}$ is a connectivity matrix, which has nd rows and $ng \times nel$ columns (Doebling et al., 1998).

Doebling et al. (1998) has parameterized the stiffness matrix of the fourth-order Bernoulli–Euler beam element in three-dimensional space by utilizing eigen decomposition. In their formulation, unusual mixed units exist. In the present study, this inconsistency of units is removed by employing the beam element with new fictitious DOFs.

3. GOAL FUNCTION

The damage identification problem is usually formulated mathematically as an inverse problem, which is generally ill-posed (Kouchmeshky et al., 2007). Usually, the problem us cast as an optimization problem in which the design variables are the members' cross-sectional properties, and the responses of the structure are known. To estimate the unknown parameters, some of the damage detection techniques, namely, output error approaches, minimize the differences between the analytical displacements and the measured ones (Hajela and Soeiro, 1990b). In these algorithms, the error vector of the ith load case has the following appearance:

$$\mathbf{R}_i = \mathbf{D}_d^a - \mathbf{D}_d^m, \tag{27}$$

where the analytical and the measured displacement vector are $\mathbf{D}_d^a$ and $\mathbf{D}_d^m$, respectively. These vectors have nd entries. Obviously, to establish the error vector, it is essential to calculate displacements analytically. Based on exact closed-form solutions, the explicit objective function is available for the case of concentrated cracks on beams (Buda and Caddemi, 2007). In this work, the equilibrium equation of the structure is employed to establish the objective function. After the damage occurs, some of the cross-sectional properties degrade. Therefore, the structure's stiffness matrix and its responses change. Consequently, the stiffness matrix of the damaged structure and its equilibrium equation will be converted into the coming shape:

$$\mathbf{K}_d = \mathbf{K} + \mathbf{\Delta K}, \tag{28}$$

$$(\mathbf{K} + \mathbf{\Delta K})\mathbf{D}_d = \mathbf{F}. \tag{29}$$

In these relationships, $\mathbf{\Delta K}$ is a $nd \times nd$ matrix, namely, perturbation matrix. This matrix shows the changes in the stiffness matrix of the healthy structure. By deploying these equations, the error vector can be obtained as below:

$$\mathbf{R}_i = (\mathbf{K} + \mathbf{\Delta K})^{-1}\mathbf{F} - \mathbf{D}_d^m. \tag{30}$$

Based on Eq. (25), $\mathbf{\Delta K}$ is calculated as follows:

$$\mathbf{\Delta K} = \mathbf{A}\boldsymbol{\delta}\widehat{\mathbf{P}}\,\mathbf{A}^T. \tag{31}$$

In this equality, $\boldsymbol{\delta}\widehat{\mathbf{P}}$ is a diagonal matrix, which has $ng \times nel$ rows and columns, and its main diagonal entries are dependent on the amounts of reduction in the cross-sectional characteristics of the members. It is worth emphasizing that $\mathbf{A}$ does not alter due to damage. According to the mentioned formulas, the goal function can be expressed in the succeeding form:

$$gf = \sum_{i=1}^{nlc} \mathbf{R}_i^T \mathbf{R}_i. \tag{32}$$

In the last relation, gf denotes the objective function, which is a function of the members' cross-sectional properties. It should be added that the number of load cases is shown by nlc. By using this goal function, the problem can be formulated as the subsequent nonlinear constrained optimization problem:

$$\begin{cases} Min\, g(diag(\boldsymbol{\delta}\widehat{\mathbf{P}})) \\ diag(\boldsymbol{\delta}\widehat{\mathbf{P}}) \leq 0, \end{cases} \tag{33}$$

where $diag(\boldsymbol{\delta}\widehat{\mathbf{P}})$ is a $ng \times nel$ vector which contains the diagonal entries of $\boldsymbol{\delta}\widehat{\mathbf{P}}$.

Mathematically, if the cross-sectional properties of the damaged structures are calculated correctly, the analytical displacements will be equal to the measured ones. As a result, the objective function will be zero. In practice, due to measurements and modeling errors this function will not exactly become zero.

4. IMPROVING THE EFFICIENCY

Up to now, the damage detection problem is formulated as a nonlinear constrained optimization problem. Note that one of the significant phases of the optimization procedures is their efficiency, and the analyzers generally endeavor to decrease the number of required computational efforts of their algorithms. Therefore, two techniques are demonstrated to reduce the consumed time of the solution procedure in the following sections.

One of the common ways to increase the efficiency of the optimization procedure is decreasing the number of design variables. For this purpose, a new approach based on the nodal equilibrium equations is proposed. By employing this method, some of the healthy members will be identified. Consequently, the number of unknowns decreases.

It is obvious that the error vector and the goal function should be computed in each iteration. To calculate them, the sum of the healthy structure's stiffness matrix and the perturbation matrix must be inverted in each cycle. There are various well-known techniques to obtain the inversion of the sum of these matrices, such as Gaussian elimination, Cholesky decomposition, LU decomposition, and so on. In addition to the aforementioned common ways, Sherman–Morrison–Woodbury formula can accurately invert the sum of two matrices. It will be proven in the present study that this approach is more efficient than the other ways. Hence, the error vector and the goal function will be constructed by utilizing this formula. In this strategy, the required arithmetic operations of the solution procedure will be reduced.

4.1. Reducing the Number of Design Variables

As previously mentioned, in damage detection problem, the cross-sectional properties of the members are the design variables. Accordingly, the number of them is equal to the number of members multiply by the number of cross-sectional properties of each element. It should be added that the proposed procedure is useful for improving the efficiency of the damage model for the cross-sectional properties of an entire element, and it can be applied only under the assumed damage mode.

It is unsuitable for the evaluation of a concentrated damage within the element length. In static damage identification problems, the structures' responses, such as displacements and strains, are known. These known parameters establish some relationships based on the equilibrium principle and constitutive laws. In general, the number of unknowns is more than known parameters. Therefore, the problem is underdeterminate, and it has more than one solution. Hence, the problem must be formulated as an optimization problem (Chou and Ghaboussi, 2001). Note that decreasing the number of unknown parameters and increasing the number of equations may remedy this problem.

In the following sections, a new technique to reduce the number of unknowns is presented. This is based on the nodal equilibrium equations of the structure, which could be written in the below form:

$$KD = F, \tag{34}$$

where the displacement and load vector are $\mathbf{D}$ and $\mathbf{F}$, respectively. They are $nd \times 1$ vector. In addition, $\mathbf{K}$ denotes the stiffness matrix, and it has $nd \times nd$ entries. The number of structure's DOFs is nd. It is obvious that the stiffness matrix is dependent on the members' cross-sectional properties. To identify the undamaged members, it is better to separate the unknown parameters from the stiffness matrix. To achieve this goal, the following formula is deployed for 3D frame:

$$\mathbf{KD} = \mathbf{T}_a\,\mathbf{A} + \mathbf{T}_t\,\mathbf{J} + \mathbf{T}_{by}\,\mathbf{I}_y + \mathbf{T}_{bz}\,\mathbf{I}_z, \tag{35}$$

The matrices, which set up the last relation, are defined as follows:

$$\mathbf{T}_a = [\mathbf{L}_1\,\mathbf{K}_{a_1}\mathbf{L}_1^T\mathbf{D}\cdots\mathbf{L}_i\,\mathbf{K}_{a_i}\mathbf{L}_i^T\mathbf{D}\cdots\mathbf{L}_{nel}\,\mathbf{K}_{a_{nel}}\mathbf{L}_{nel}^T\mathbf{D}], \tag{36}$$

$$\mathbf{T}_t = [\mathbf{L}_1\,\mathbf{K}_{t_1}\mathbf{L}_1^T\mathbf{D}\cdots\mathbf{L}_i\,\mathbf{K}_{t_i}\mathbf{L}_i^T\mathbf{D}\cdots\mathbf{L}_{nel}\,\mathbf{K}_{t_{nel}}\mathbf{L}_{nel}^T\mathbf{D}], \tag{37}$$

$$\mathbf{T}_{by} = [\mathbf{L}_1\mathbf{K}_{by_1}\mathbf{L}_1^T\mathbf{D}\cdots\mathbf{L}_i\,\mathbf{K}_{by_i}\mathbf{L}_i^T\mathbf{D}\cdots\mathbf{L}_{nel}\,\mathbf{K}_{by_{nel}}\mathbf{L}_{nel}^T\mathbf{D}], \tag{38}$$

$$\mathbf{T}_{bz} = [\mathbf{L}_1\,\mathbf{K}_{bz_1}\mathbf{L}_1^T\mathbf{D}\cdots\mathbf{L}_i\,\mathbf{K}_{bz_i}\mathbf{L}_i^T\mathbf{D}\cdots\mathbf{L}_{nel}\,\mathbf{K}_{bz_{nel}}\mathbf{L}_{nel}^T\mathbf{D}]. \tag{39}$$

In addition, the subsequent vectors include the members' cross-sectional properties:

$$\mathbf{A} = \{A_1\ A_2\ \cdots\ A_{nel}\}, \tag{40}$$

$$\mathbf{I}_x = \{I_{x_1}\ I_{x_2}\ \cdots\ I_{x_{nel}}\}^T, \tag{41}$$

$$\mathbf{I}_y = \{I_{y_1}\ I_{y_2}\ \cdots\ I_{y_{nel}}\}^T, \tag{42}$$

$$\mathbf{I}_z = \{I_{z_1}\ I_{z_2}\ \cdots\ I_{z_{nel}}\}^T. \tag{43}$$

In these equalities, $\mathbf{T}_a$, $\mathbf{T}_t$, $\mathbf{T}_{by}$, and $\mathbf{T}_{bz}$ are $nd \times nel$ rectangular matrices. The number of DOFs and members are shown by nd and nel, respectively. Moreover, the entries of $\mathbf{I}_x$, $\mathbf{I}_y$, and $\mathbf{I}_z$ are the moments of inertia, and $\mathbf{A}$ includes cross-sectional areas. The connectivity matrix of the ith element is shown by $\mathbf{L}_i$. In 3D frames, this matrix has nd rows and 12 columns. Note that number of DOFs of a 3D frame

element is equal to 12. Furthermore, $\mathbf{K}_{a_i}$, $\mathbf{K}_{t_i}$, $\mathbf{K}_{by_i}$, and $\mathbf{K}_{bz_i}$ are 12×12 matrices, which can build the global stiffness matrix of ith element in the next shape:

$$\mathbf{K}_{G_i} = A_i\mathbf{K}_{a_i} + J_i\mathbf{K}_{t_i} + I_{y_i}\mathbf{K}_{by_i} + I_{z_i}\mathbf{K}_{bz_i}, \tag{44}$$

The ith element's stiffness matrix in global coordinates is demonstrated by $\mathbf{K}_{G_i}$. As previously mentioned, the damage is modeled by reducing the cross-sectional properties. As a result, the stiffness matrix and the displacement vector of the structure will be changed. Therefore, the equilibrium equation of the structure will be written in below form:

$$\mathbf{K}_d\mathbf{D}_d = \mathbf{F}. \tag{45}$$

In this equality, the damaged structural stiffness matrix and the displacement vector are shown by $\mathbf{K}_d$ and $\mathbf{D}_d$, respectively. To identify the healthy members, Eq. (45) should be converted into the form of Eq. (35), which clearly separates the cross-sectional properties of each element from the stiffness matrix. For this purpose, $\mathbf{D}_d$ must be used instead of $\mathbf{D}$. It is worth emphasizing that $\mathbf{K}_{a_i}$, $\mathbf{K}_{t_i}$, $\mathbf{K}_{by_i}$, and $\mathbf{K}_{bz_i}$ are the same in damaged and undamaged structures.

In fact, Eqs. (34) and (45) are system of equations. Each equation of them is a nodal force or moment equilibrium equation in translational or rotational direction. As it is shown in Eq. (35), equations related to a specific node are dependent on the cross-sectional properties among the elements connected to the mentioned node. In damaged structure, the cross-sectional properties are unknown. If these parameters are estimated correctly, the system of nodal equilibrium equations of the unhealthy structure will be satisfied. In practice, only few members within the structure deteriorate due to damage, and others remain healthy. To identify the undamaged ones, it is first supposed that all the members are unharmed. In other words, the cross-sectional properties of the healthy structures are employed in Eq. (45). If all the members connected to the specific node are undamaged, the nodal equilibrium equations of the mentioned node will be satisfied by inserting the healthy cross-sectional properties into Eq. (45). By this mean, the nodes whose elements are undamaged can be detected. Afterward, the healthy members can be easily identified by finding the members related to these nodes. It is obvious that the proposed approach cannot detect the healthy elements, which are connected to two damaged nodes. By employing this strategy, the number of unknowns is reduced, and the efficiency of the optimization procedure improves. On the other hand, deploying the aforementioned form of the equilibrium equations, instead of the common way, will reduce the complexity of the computer programming. It should be added that the equilibrium equation of the 2D frame in the shape of Eq. (35) will be given in Appendix B.

4.2. Constructing the Goal Function

As it was discussed earlier, the damaged structural stiffness matrix is the sum of the perturbation matrix and the undamaged structure's stiffness matrix. Clearly, the perturbation matrix is a function of unknown parameters. In damage detection

algorithm, the sum of these matrices must be essentially inverted in each cycle of the solution procedure.

Sherman–Morrison–Woodbury formula is an accurate technique to compute the inversion of the sum of two matrices (Hager, 1989; Henderson and Searle, 1981). This identity has been utilized in different branch of structural and electrical engineering. In addition, it has been used in solving the differential equations, sensitivity analysis in linear programming, and quasi-Newton approaches (Hager, 1989). However, the mentioned relationship has not been employed in the damage detection of frames yet. In this paper, the stated method will be applied to set up the error vector and the objective function of the problem. To achieve this goal, the stiffness matrix of the structure is perturbed due to damage and $\mathbf{\Delta K}$ demonstrates the amount of changes in this matrix. By applying the Sherman–Morrison–Woodbury formula, the damaged structural stiffness matrix can be inverted as follows:

$$(\mathbf{K} + \mathbf{\Delta K})^{-1} = (\mathbf{K} + \mathbf{U}\,\mathbf{H}^{-1}\,\mathbf{V})^{-1} = \mathbf{K}^{-1} - \mathbf{K}^{-1}\mathbf{U}(\mathbf{H} + \mathbf{V}\,\mathbf{K}^{-1}\,\mathbf{U})^{-1}\mathbf{V}\,\mathbf{K}^{-1}. \tag{46}$$

In this relationship, $\mathbf{\Delta K}$ is equal to $(\mathbf{U}\,\mathbf{H}^{-1}\,\mathbf{V})$. Based on Equation (31), $\mathbf{U}$, $\mathbf{V}$, and $\mathbf{H}$ are clearly $\mathbf{A}$, $\mathbf{A}^T$, and $\boldsymbol{\delta}\widehat{\mathbf{P}}^{-1}$, respectively. It should be added that $(\mathbf{H} + \mathbf{V}\,\mathbf{K}^{-1}\mathbf{U})$ is named capacitance matrix. Number of rows and columns of this matrix are dependent on the dimensions of $\mathbf{U}$, $\mathbf{V}$, and $\mathbf{H}$. For being Eq. (46) computable, $(\mathbf{H} + \mathbf{V}\,\mathbf{K}^{-1}\mathbf{U})$, $\mathbf{H}$, and $\mathbf{K}$ must be invertible. On the other hand, it is not necessary for $\mathbf{\Delta K}$ to have inverse. It should be reminded that the stable structural stiffness matrix is always invertible.

As previously mentioned, Sherman–Morrison–Woodbury formula is employed to establish the goal function and the error vector in each cycle. When the rank of the perturbation matrix is less than the stiffness matrix, the effort involved in computing $(\mathbf{K} + \mathbf{\Delta K})^{-1}$ is small relative to the effort required to invert this matrix by classical methods, such as Guassian elimination, Cholesky decomposition and LU decomposition. To make the rank of $\mathbf{\Delta K}$ smaller than $\mathbf{K}$, healthy members are identified by utilizing the technique in the previous section. After detecting the undamaged members, the columns of $\mathbf{A}$ matrix, which are related to these members will be eliminated. Consequently, the number of columns of this matrix will be reduced. In the following lines, $\mathbf{A}_m$ denotes the new obtained matrix which has $nrm \times ng$ columns and nd rows. The number of damaged members is equal to nrm. In addition, the rows and columns of $\boldsymbol{\delta}\widehat{\mathbf{P}}$ related to the damaged members will be removed. Hence, a new diagonal matrix, which is called $\boldsymbol{\delta}\widehat{\mathbf{P}}_m$, will be obtained. This matrix has $nrm \times ng$ rows and columns. Afterwards, $\mathbf{A}$ and $\boldsymbol{\delta}\widehat{\mathbf{P}}$ are substituted by $\mathbf{A}_m$ and $\boldsymbol{\delta}\widehat{\mathbf{P}}_m$, respectively In this way, $\mathbf{\Delta K}$ is calculated as below:

$$\mathbf{\Delta K} = \mathbf{A}_m \boldsymbol{\delta}\widehat{\mathbf{P}}_m\,\mathbf{A}_m^T. \tag{47}$$

Based on this equality, the following expression can be written as

$$\mathbf{\Delta K} = \mathbf{U}\mathbf{H}^{-1}\mathbf{V} = \mathbf{A}_m \boldsymbol{\delta}\widehat{\mathbf{P}}_m\,\mathbf{A}_m^T. \tag{48}$$

To invert $(\mathbf{K} + \mathbf{\Delta K})$, it is essential to reverse $\boldsymbol{\delta}\widehat{\mathbf{P}}_m$. To achieve this, its main diagonal entries must be inverted since this matrix is a diagonal matrix. It is worth

emphasizing that some healthy members may sometimes be identified mistakenly as damaged ones by utilizing the tactic proposed in the previous section. In this case, the aforesaid matrix does not have an inverse. To solve this problem, a lower bound, which is relatively small to the cross-sectional properties, is introduced on variables. These bounds show a very small reduction in cross-sectional properties of the damaged members. In this way, $\delta\widehat{\mathbf{P}}_m$ is always invertible. Deploying Eqs. (46) and (48) leads to the subsequent result:

$$\boldsymbol{D}_{\mathrm{d}}^{\mathrm{a}} = (\boldsymbol{K}^{-1} - \boldsymbol{K}^{-1}\boldsymbol{A}_{\mathrm{m}}(\delta\widehat{\boldsymbol{P}}_{\mathrm{m}}^{-1} + \boldsymbol{A}_{\mathrm{m}}^{T}\boldsymbol{K}^{-1}\boldsymbol{A}_{\mathrm{m}})^{-1}\boldsymbol{A}_{\mathrm{m}}^{T}\boldsymbol{K}^{-1})\boldsymbol{F}. \tag{49}$$

This relation can be rewritten in the following form:

$$\mathbf{D}_{d}^{\mathrm{a}} = \mathbf{D} - \mathbf{K}^{-1}\mathbf{A}_{m}(\delta\widehat{\mathbf{P}}_{m}^{-1} + \mathbf{A}_{m}^{T}\mathbf{K}^{-1}\mathbf{A}_{m})^{-1}\mathbf{A}_{m}^{T}\mathbf{D}. \tag{50}$$

By employing the last equations, the error vector is obtained as follows:

$$\mathbf{R}_{i} = (\mathbf{D} - \mathbf{K}^{-1}\mathbf{A}_{m}(\delta\widehat{\mathbf{P}}_{m}^{-1} + \mathbf{A}_{m}^{T}\mathbf{K}^{-1}\mathbf{A}_{m})^{-1}\mathbf{A}_{m}^{T}\mathbf{D}) - \mathbf{D}_{d}^{m}. \tag{51}$$

Afterward, the objective function is established, and the unknown parameters will be estimated by minimizing the goal function. Note that Sherman–Morrison–Woodbury formula has various forms, which will be introduced in Appendix C.

5. NUMERICAL EXAMPLES

In this section, several numerical examples are presented to illustrate the robustness of the proposed technique in damage detection of frames. First, a damage scenario is presumed for each structure. Then, the damaged structures' responses are obtained by utilizing the structural analysis methods, instead of measuring them. Afterward, two algorithms are deployed to detect the magnitude and the location of damage in frames, and the results are shown in tables. It should be noted that these methods are not able to localize the concentrated damage because damage is modeled as a reduction in cross-sectional properties of members. However, this limitation can be to some extend remedied by successively subdividing the members. To establish the objective function, Sherman–Morrison–Woodbury formula is applied in the first approach, whereas the second algorithm employs LU decomposition. It is clear that LU decomposition is a common technique to invert matrices. This tactic factorizes a matrix as a product of a lower triangular matrix and an upper one and then calculates inversion of the initial matrix. It should be mentioned that the second tactic is used along with the first one to demonstrate the efficiency of the algorithm, in which Sherman–Morrison–Woodbury formula is applied. To compare the efficiency of these two approaches, an efficiency index is defined. This guide is based on the consumed time of each algorithm for converging to the solution. The following expression mathematically demonstrates the index:

$$IT_{i} = \frac{T_{\min}}{T_{i}} \times 100 \tag{52}$$

where $T_{\min}$ denotes the consumed time of the fastest method, and T_i is the consumed time of the ith formulation. It is worth emphasizing that simple load cases are utilized in the following numerical examples. Other researchers have comprehensively studied the characteristics of the appropriate load cases for damage identification of structures (Bakhtiari-Nejad et al., 2005; Kouchmeshky et al., 2007; Liu and Chian, 1997; Sanayei and Onipede, 1991). Moreover, the conditions of the optimization problem are similar in both schemes. To detect the location and the severity of damage in the following examples, a Fortran program has been implemented by the authors.

5.1. Planar Eight-Members Frame

A two-storey frame is shown in Fig. 3 (Saliani, 1999). Its number of DOFs is 18. This frame is an indeterminate structure.

The frame's cross-sectional areas and moments of inertia are $200\,\mathrm{mm}^2$ and $1066.7\,\mathrm{mm}^4$, respectively. Furthermore, the Young's modulus is $2 \times 10^6\,\mathrm{kg/cm}^2$. The cross-sectional properties of members 2 and 6 deteriorate due to damage. The damaged properties are shown in Table 1. As previously mentioned, a simple load case is employed. Here, the first and second storey's applied loads at the horizontal DOFs are chosen to be 1 and 2 kg, respectively. In addition, the first and second storey's vertical DOFs are subjected to the loads with the value of -1 and -3 kg, respectively. Besides, the nodal moments of the first storey are $1\,\mathrm{kg}\cdot\mathrm{cm}$, and those of the second storey are $2\,\mathrm{kg}\cdot\mathrm{cm}$.

At the first stage, the damaged members are identified by utilizing the tactic proposed in Section 4.1. Then, the magnitude and the location of damage are detected by deploying the two mentioned algorithms. The results are illustrated in Table 1.

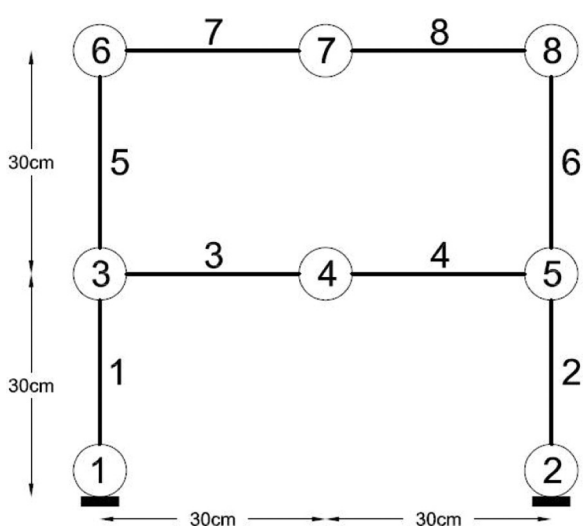

Figure 3 Planar eight member frame.

Table 1 The results of damage detection in planar eight-members frame

	Cross-sectional areas				Moment of inertias			
Element	Before damage	After damage	Estimated by first method	Estimated by second method	Before damage	After damage	Estimated by first method	Estimated by second method
2	200	150	150	150	1066.7	700	700	700
6	200	170	170	170	1066.7	800	800	800

Table 2 The results of each iteration for damage detection of planar eight-members frame

	Element 2		Element 6	
Iteration	Cross-sectional area	Moment of inertia	Cross-sectional area	Moment of inertia
1	198	1056.03	198	1056.03
2	134.36	611.55	164.45	735.30
3	148.46	693.81	169.70	794.85
4	149.98	699.97	169.99	799.96
5	150	700	170	800

The results of each iteration in damage detection procedure are presented in Table 2.

It is obvious that both techniques correctly estimate the damaged members' cross-sectional properties. Note that these strategies are able to converge to the exact solution because they utilize accurate approaches to invert the sum of the healthy structural stiffness matrix and the perturbation matrix.

Since only two members are identified as damaged ones, the rank of the perturbation matrix is less than the stiffness matrix. Consequently, Sherman–Morrison–Woodbury formula requires fewer arithmetic operations than LU decomposition. It is worth emphasizing that each algorithm's consumed time is infinitesimal, because this frame is very small. As a result, the difference between the consumed time of these approaches is only a fraction of hundredth of a second. Therefore, the efficiency indexes are not mentioned.

5.2. Planar Nine-Members Frame

A planar nine-member frame with 18 DOFs is demonstrated in Fig. 4. Previously, other researchers have identified damage in this 2D frame (Saliani, 1999). The cross-sectional areas and the moments of inertia of this structure are $80\,\text{cm}^2$ and $7800\,\text{cm}^4$, respectively. Moreover, Young's modulus is $2 \times 10^6\,\text{kg/cm}^2$.

The cross-sectional properties of members 3 and 4 deteriorate due to damage. To detect the magnitude and the location of damage, the load applied at horizontal and vertical DOFs is chosen to be -100 and $-150\,\text{kg}$, respectively. In addition, the nodal moments are $2000\,\text{kg}\cdot\text{cm}$.

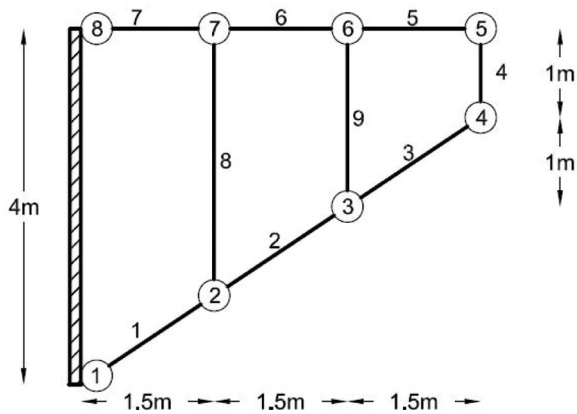

Figure 4 Planar nine-member frame.

Table 3 The results of damage detection in planar nine-members frame

	Cross-sectional areas				Moment of inertias			
Element	Before damage	After damage	Estimated by first method	Estimated by second method	Before damage	After damage	Estimated by first method	Estimated by second method
3	80	75	75	75	7800	6400	6400	6400
4	80	65	65	65	7800	6500	6500	6500

By employing the tactic proposed in Section 4.1, damaged members are identified. Then, these members' cross-sectional areas and moments of inertia are calculated by deploying the two aforementioned techniques. The results are presented in Table 3.

The results of each iteration in damage detection procedure are presented in Table 4.

In this example, the cross-sectional properties are calculated correctly. As mentioned so far, both formulations use an accurate technique to invert the sum of two matrices. Note that the first tactic needs less computational efforts than the second one. Since the structure is relatively small, the consumed time of both

Table 4 The results of each iteration for damage detection of planar nine-members frame

	Element 3		Element 4	
Iteration	Cross-sectional area	Moment of inertia	Cross-sectional area	Moment of inertia
1	79.20	7722	79.20	7722
2	75.24	6505.63	67.84	5869.99
3	75.02	6399.36	65.16	6441.13
4	75	6400.01	65	6499.47
5	75	6400	65	6500

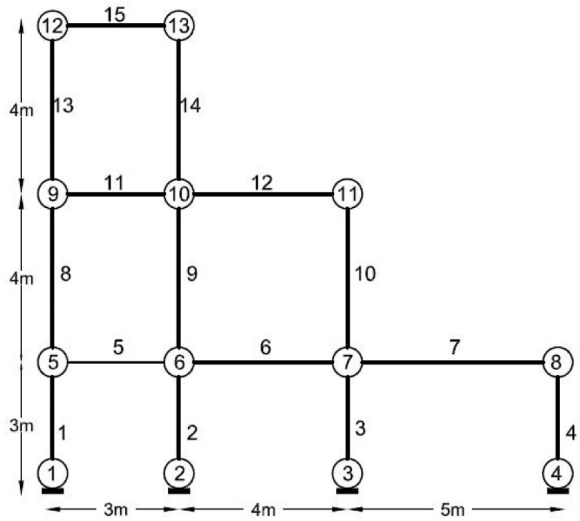

Figure 5 Planar 15-member frame.

algorithms is approximately equal. Consequently, the efficiency indexes are not mentioned.

5.3. Planar 15-Members Frame

A 2D frame, which has 3 storey and 27 DOFs is shown in Fig. 5. The members' cross-sectional areas and moments of inertia are $50\,\text{cm}^2$ and $2000\,\text{cm}^4$, respectively. In addition, the longitudinal elasticity (Young) modulus is $2 \times 10^6\,\text{kg/cm}^2$. It should be mentioned that other researchers have assessed damage in this frame (Saliani, 1999).

A damage scenario is presumed, and the proposed algorithms are deployed to detect the magnitude and location of damage. The cross-sectional properties of members 1, 8, and 13 are reduced due to damage. At first stage, undamaged members are identified. Then, the cross-sectional properties are calculated. To assess damage, the frame's nodes are subjected to the horizontal loads with the value of 100 kg. In addition, nodal vertical loads and moments are $-120\,\text{kg}$ and $250\,\text{kg}\cdot\text{cm}$, respectively. The results are listed in Table 5. It should be added that only the cross-sectional properties of the damaged members are listed in the next table.

The findings prove that both algorithms are able to calculate the cross-sectional properties correctly. This is because both schemes utilize accurate techniques to invert the sum of the stiffness matrix and the perturbation matrix.

To compare the efficiency of the proposed schemes, the efficiency index is utilized. It is worth emphasizing that the consumed time of these approaches are relatively very small. However, their differences are completely tangible. The efficiency indexes of the presented algorithms are 100 and 48.27, respectively. Consequently, the first technique is faster than the second one. As previously mentioned, Sherman–Morrison–Woodbury formula, which is used in the first approach, requires less computational efforts than LU decomposition to invert

Table 5 The results of damage detection in planar 15-members frame

	Cross-sectional areas				Moment of inertias			
Element	Before damage	After damage	Estimated by first method	Estimated by second method	Before damage	After damage	Estimated by first method	Estimated by second method
1	50	40	40	40	2000	1700	1700	1700
8	50	40	40	40	2000	1750	1750	1750
13	50	40	40	40	2000	1800	1800	1800

matrices. It should be reminded that the lesser the rank of $\mathbf{\Delta K}$ is, in comparison with $\mathbf{K}$, the smaller amount arithmetic operations the first formulation needs.

5.4. 3D 13-Members Frame

A 3D frame with 13 members and 36 DOFs is illustrated in Fig. 6. All of its supports are fixed. It should be added that the entire members are specified. The nodes are numbered in clockwise direction, and the upper node of the first member is node 1. The cross-sectional areas of this structure are 40 cm^2, and the moments of inertia are 2000, 700, and 1500 cm^4. Furthermore, Young's modulus and Poisson's modulus are 2×10^6 kg/cm^2 and 0.29, respectively.

After the damage occurrence, it is assumed that the cross-sectional area of member 5 is reduced to 36 cm^2. Moreover, its moments of inertia decrease to 1620, 567, and 1215 cm^4, respectively. To assess damage in this structure, the load case presented in Table 6 is utilized. By deploying the proposed technique in Section 4.1,

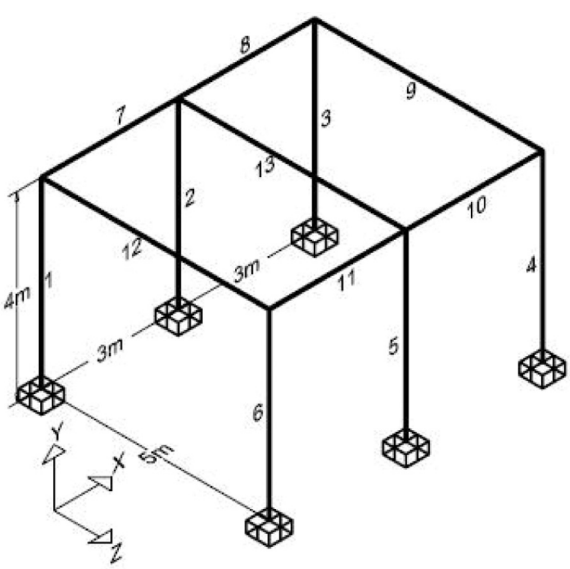

Figure 6 3D 13-member frame.

Table 6 Load case applied to 3D 13-member frame

Nodes	Load in X direction (kg)	Load in Y direction (kg)	Load in Z direction (kg)	Moment in X direction (kg.cm)	Moment in Y direction (kg.cm)	Moment in Z direction (kg.cm)
1	1000	−2000	1000	1000	−900	0
2	1000	−2000	1000	1000	−900	0
3	1000	−2000	1000	1000	−900	0
4	2000	−2000	1000	1000	−900	0
5	2000	−2000	1000	1000	−900	0
6	2000	−2000	1000	1000	−900	0

the damaged member can be identified. The two suggested algorithms calculate the cross-sectional properties correctly.

By comparing the efficiency indexes of the presented methods, the capable strategy can be determined. According to the calculation, the efficiency indexes are 100 and 23.33, respectively. Once again, the first algorithm is faster than the second one.

5.5. 3D 29-Members Frame

A 3D frame with 29 member and 84 DOFs is demonstrated in Fig. 7. All of structural supports are fixed, and its nodes are numbered. The members' cross-sectional areas are 50 cm^2, and the moments of inertia are 2500, 1000, and 1500 cm^4, correspondingly. In addition, Young's modulus and Poisson's modulus are 2×10^6 kg/cm^2 and 0.29, respectively.

It is assumed that the cross-sectional properties of member 4 (its first node is node 4, and its second node is 10) and member 6 (its first node is node 6, and its second one is node 12) degrades due to damage. The cross-sectional area of the fourth member decreases to 35 cm^2 after the damage occurrence, and its moments of inertia decrease to 1800, 600, and 1100 cm^4, respectively. Besides, after the occurrence of damage, the sixth member's cross-sectional area and moments of inertia will become 40 cm^2 and 2000, 700, and 1300 cm^4, correspondingly. It should be noted that the applied load pattern to detect the magnitude and location of damage is shown in Table 7.

By utilizing the aforementioned load pattern and investigating the nodal equilibrium equations, the damaged members can be detected. Afterward, the presented algorithms are employed to estimate the magnitude of damage. The findings demonstrate that both techniques calculate the cross-sectional properties of the damaged members correctly.

It should be added that the efficiency indexes of the proposed technique are 100 and 7.85. As a result, the first formulation is much faster and requires lesser arithmetic operations than the second tactic. Comparing this example with the previous ones, the difference between the suggested methods' index is bigger, because the rank of $\mathbf{\Delta K}$ is much smaller than the structural stiffness matrix.

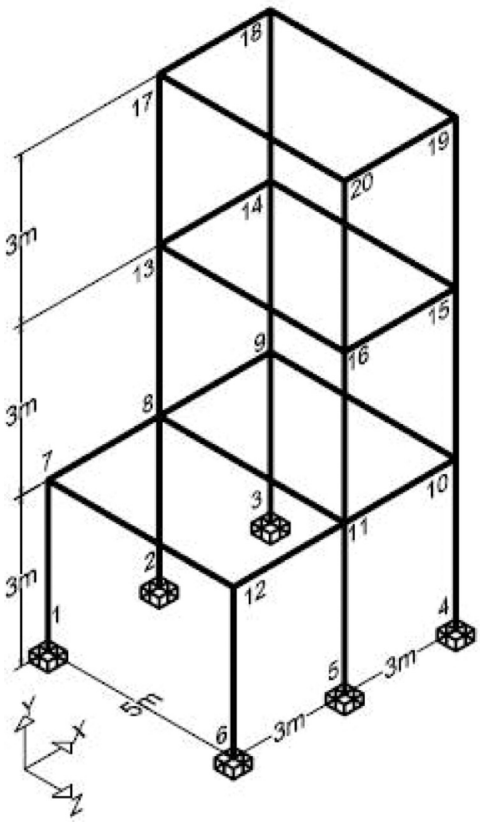

Figure 7 3D 29-member frame.

Table 7 Load case applied to 3D 29-member frame

Nodes	Load in X direction (kg)	Load in Y direction (kg)	Load in Z direction (kg)	Moment in X direction (kg · cm)	Moment in Y direction (kg · cm)	Moment in Z direction (kg · cm)
7	−1000	−3000	−2000	1000	−900	0
8	−1000	−3000	−2000	1000	−900	0
9	−1000	−3000	−2000	1000	−900	0
10	−1000	−3000	−2000	1000	−900	0
11	−1000	−3000	−2000	1000	−900	0
12	−1000	−3000	−2000	1000	−900	0
13	−1000	−2000	−2000	1000	−900	0

6. CONCLUSION

In this article, an algorithm for static damage detection of 3D and 2D frames was proposed. The presented formulations lead to a nonlinear constrained optimization problem, in which the differences between the analytical and measured

displacements are minimized. To formulate the problem, a new technique to parameterize the global stiffness matrix was presented. This approach employs the eigen decomposition of the local elemental stiffness matrix. In addition, it is necessary to compute the analytical displacements to establish the objective function. According to the solution procedure, the sum of healthy structural stiffness matrix and the perturbation matrix should be inverted. To achieve this goal, Sherman–Morrison–Woodbury formula is employed. Prior to the outset of the optimization process, the number of design variables, cross-sectional properties, is reduced by utilizing the new suggested tactic. This technique is based on the nodal equilibrium equations.

To find the robustness of the proposed algorithm, several numerical tests were performed. To demonstrate the efficiency of this approach, another method, which uses LU decomposition, instead of Sherman–Morrison–Woodbury formula, was employed for solving numerical samples. Based on the findings, it can be concluded that both approaches are able to detect the location and the magnitude of damage successfully. However, it is proven that the first technique is faster and needs fewer arithmetic operations than the second one.

It is worth mentioning that the accuracy of the presented algorithms is dependent on the applied load cases, and the consumed time of each method is related to the topology and geometry of the structure, the damage scenario, and the load pattern. Generally in small frames, although the first technique requires fewer arithmetic operations than the second one, the difference between their consumed time is a fraction of hundredth of a second. The smaller the damage zone is, in comparison with the structure, the lesser the rank of the perturbation matrix becomes. In this case, the first method requires much fewer computational efforts than the second one.

REFERENCES

Abdo, M. A. B. (2012). Parametric study of using only static response in structural damage detection. *Engineering Structures* 34:124–131.

Akgun, M. A., Ju, F. D. (1990). Damage diagnosis in frame structures with a dynamic response method. *Mechanics of Structures and Machines* 18(2):175–196.

Aktas, E., Moses, F. (1998). Reduced basis eigenvalue solutions for damaged structures. *Mechanics of Structures and Machines* 26(1):63–79.

Alves, M. (2001). Measurement of ductile material damage. *Mechanics of Structures and Machines* 29(4):451–476.

Bakhtiari-Nejad, F., Rahai, A., Esfandiari, A. (2005). A structural damage detection method using static noisy data. *Engineering Structures* 27:1784–1793.

Banan, M. R., Banan, M. R., Hjelmstad, K. D. (1994a). Parameter estimation of structures from static response, I: Computational aspects. *Journal of Structural Engineering* 120(11):3243–3258.

Banan, M. R., Banan, M. R., Hjelmstad, K. D. (1994b). Parameter estimation of structures from static response, II: Numerical simulation. *Journal of Structural Engineering* 120(11):3259–3283.

Buda, G., Caddemi, S. (2007). Identification of concentrated damage in Euler-Bernoulli beam under static loads. *Journal of Engineering Mechanics-ASCE* 133(8):942–956.

Caddemi, S., Calio, I. (2013). The exact explicit dynamic stiffness matrix of the multi-cracked Euler-Bernoulli beam and applications to damaged frame structures. *Journal of Sound and Vibrations* 332(12):3049–3063.

Caddemi, S., Greco, A. (2006). The influence of instrumental errors on the static identification of damage parameters for elastic beams. *Computer & Structures* 84:1696–1708.

Caddemi, S., Morassi, A. (2007). Crack detection in elastic beams by static measurements. *Journal of Engineering Mechanics* 44(16):5301–5315.

Caddemi, S., Morassi, A. (2011). Detecting multiple open cracks in elastic beams by static tests. *Journal of Engineering Mechanics-ASCE* 137(2):113–124.

Calio, I., Greco, A. (2013). Free vibrations of Timoshenko beam-columns on Pasternak foundations. *Journal of Vibration and Control* 19(5):686–696.

Carden, E. P., Fanning, P. (2004). Vibration based condition monitoring: A review. *Structural Health Monitoring* 3(4):355–377.

Chou, J. H., Ghaboussi, J. (2001). Genetic algorithm in structural damage detection. *Computers and Structures* 79:1335–1353.

Doebling, S. W., Peterson, L. D., Alvin, K. F. (1998). Experimental determination of local structural stiffness by disassembly of measured flexibility matrices. *Journal of Vibration and Acoustics* 120:949–957.

Dong, C., Ding, H., Gao, S. (2002). A method for recognition and location of structural damage. *Mechanics of Structures and Machines* 30(2):193–201.

Hager, W. W. (1989). Updating the inverse of a matrix. *SIAM Review* 31(2):221–239.

Hajela, P., Soeiro, F. J. (1990a). Structural damage detection based on static and modal analysis. *AIAA Journal* 28(6):1110–1115.

Hajela, P., Soeiro, F. J. (1990b). Recent development in damage detection based on system identification methods. *Structural Optimization* 2:1–10.

Henderson, H. V., Searle, S. R. (1981). On deriving the inverse of a sum of matrices. *SIAM Review* 23(1):53–60.

Hjelmstad, K. D., Shin, S. (1997). Damage detection and assessment of structures from static response. *Journal of Engineering Mechanics* 123(6):568–576.

Kouchmeshky, B., Aquino, W., Bongard, J. C., Lipson, H. (2007). Co-evolutionary algorithm for structural damage identification using minimal physical testing. *International Journal For Numerical Methods in Engineering* 69:1085–1107.

Liu, P. L., Chian, C. C. (1997). Parameter identification of truss structures using static strains. *Journal of Structural Engineering* 123(7):927–933.

Ramamurti, V., Neogy, S. (1998). Effect of cracks on the natural frequency of the cantilevered plates—a Rayleigh-Ritz solution. *Mechanics of Structures and Machines* 26(2):131–143.

Rezaiee-Pajand, M., Aftabi Sani, A. (2008). Truss damage detection utilizing pseudo-dual simplex method. *International Journal of Engineering Science (IUST-in Persian)* 19(8):77–87.

Rezaiee-Pajand, M., Moayyedian, M. (2004). *Finite Element Theory* (in Persian). Mashhad, Iran: Islamic Azad University Publication.

Rezaiee-Pajand, M., Saliani, M. (2004). Damage assessment of plane trusses by static finite element method. *Journal of Tehran University College of Engineering (in Persian)* 38(6):759–775.

Saliani, M. (1999). *Damage Detection of Plane Structures by Static Finite Element Method* (in Persian). Master Thesis. Ferdowsi University of Mashhad, Iran.

Sanayei, M., Nelson, R. B. (1986). *Identification of Structural Element Stiffness from Incomplete Static Test Data*. Society of Automotive Engineering, Technical Paper, SAE.

Sanayei, M., Onipede, O. (1991). Damage assessment of structures using static test data. *AIAA Journal* 29:1174–1179.

Sanayei, M., Saletnik, M. J. (1996a). Parameter estimation of structures from static strain measurements I. *Journal of Structural Engineering ASCE* 122(5):555–562.

Sanayei, M., Saletnik, M. J. (1996b). Parameter estimation of structures from static strain measurements II: Error sensitivity analysis. *Journal of Structural Engineering ASCE* 122(5):563–572.

Sheena, Z., Unger, A., Zalmanovich, A. (1982). Theoretical stiffness matrix correction by static test results. *Israel Journal of Technology* 20:245–253.

Shenton III, H. W., Hu, X. (2006). Damage identification based on dead load redistribution: Methodology. *Journal of Structural Engineering* 132(8):1254–1263.

Yang, Q. W., Sun, B. X. (2010). Structural damage localization and quantification using static test data. *Structural Health Monitoring* 10(4):381–389.

APPENDIX A

Eigenvalues, Eigenvectors, and the Transformation Matrices of the 3D and 2D Frame Elements

The eigenvectors, eigenvalues, and the transformation matrix of the 2D frame element have the succeeding forms:

$$\hat{\boldsymbol{\lambda}} = \begin{Bmatrix} \frac{2EI_z}{L^3} \\ \frac{30EI_z}{L^3} \\ \frac{2AE}{L} \end{Bmatrix}, \quad \hat{\boldsymbol{\kappa}} = \begin{bmatrix} 0 & 0 & \frac{-1}{\sqrt{2}} \\ 0 & \frac{2}{\sqrt{10}} & 0 \\ \frac{-1}{\sqrt{2}} & \frac{1}{\sqrt{10}} & 0 \\ 0 & 0 & \frac{1}{\sqrt{2}} \\ 0 & \frac{-2}{\sqrt{10}} & 0 \\ \frac{1}{\sqrt{2}} & \frac{1}{\sqrt{10}} & 0 \end{bmatrix}, \tag{A.1}$$

$$\mathbf{Q} = \begin{bmatrix} 1 & 0 & 0 & 0 & 0 & 0 \\ 0 & 1 & 0 & 0 & 0 & 0 \\ 0 & 0 & L & 0 & 0 & 0 \\ 0 & 0 & 0 & 1 & 0 & 0 \\ 0 & 0 & 0 & 0 & 1 & 0 \\ 0 & 0 & 0 & 0 & 0 & L \end{bmatrix}. \tag{A.2}$$

In addition, the eigenvectors, nonzero eigenvalues, and the transformation matrix of the 3D frame element can be expressed as below:

$$\hat{\boldsymbol{\lambda}} = \begin{Bmatrix} \frac{2EI_y}{L^3} \\ \frac{30EI_y}{L^3} \\ \frac{2EI_z}{L^3} \\ \frac{30EI_z}{L^3} \\ \frac{2AE}{L} \\ \frac{2GJ}{L} \end{Bmatrix}, \quad \hat{\kappa} = \begin{bmatrix} 0 & 0 & 0 & 0 & \frac{-1}{\sqrt{2}} & 0 \\ 0 & 0 & 0 & \frac{2}{\sqrt{10}} & 0 & 0 \\ 0 & \frac{-2}{\sqrt{10}} & 0 & 0 & 0 & 0 \\ 0 & 0 & 0 & 0 & 0 & \frac{-1}{\sqrt{2}} \\ \frac{-1}{\sqrt{2}} & \frac{1}{\sqrt{10}} & 0 & 0 & 0 & 0 \\ 0 & 0 & \frac{-1}{\sqrt{2}} & \frac{1}{\sqrt{10}} & 0 & 0 \\ 0 & 0 & 0 & 0 & \frac{1}{\sqrt{2}} & 0 \\ 0 & 0 & 0 & \frac{-2}{\sqrt{10}} & 0 & 0 \\ 0 & \frac{2}{\sqrt{10}} & 0 & 0 & 0 & 0 \\ 0 & 0 & 0 & 0 & 0 & \frac{1}{\sqrt{2}} \\ \frac{1}{\sqrt{2}} & \frac{1}{\sqrt{10}} & 0 & 0 & 0 & 0 \\ 0 & 0 & \frac{1}{\sqrt{2}} & \frac{1}{\sqrt{10}} & 0 & 0 \end{bmatrix}, \tag{A.3}$$

$$\mathbf{Q} = \begin{bmatrix} 1 & 0 & 0 & 0 & 0 & 0 & 0 & 0 & 0 & 0 & 0 & 0 \\ 0 & 1 & 0 & 0 & 0 & 0 & 0 & 0 & 0 & 0 & 0 & 0 \\ 0 & 0 & 1 & 0 & 0 & 0 & 0 & 0 & 0 & 0 & 0 & 0 \\ 0 & 0 & 0 & 1 & 0 & 0 & 0 & 0 & 0 & 0 & 0 & 0 \\ 0 & 0 & 0 & 0 & L & 0 & 0 & 0 & 0 & 0 & 0 & 0 \\ 0 & 0 & 0 & 0 & 0 & L & 0 & 0 & 0 & 0 & 0 & 0 \\ 0 & 0 & 0 & 0 & 0 & 0 & 1 & 0 & 0 & 0 & 0 & 0 \\ 0 & 0 & 0 & 0 & 0 & 0 & 0 & 1 & 0 & 0 & 0 & 0 \\ 0 & 0 & 0 & 0 & 0 & 0 & 0 & 0 & 1 & 0 & 0 & 0 \\ 0 & 0 & 0 & 0 & 0 & 0 & 0 & 0 & 0 & 1 & 0 & 0 \\ 0 & 0 & 0 & 0 & 0 & 0 & 0 & 0 & 0 & 0 & L & 0 \\ 0 & 0 & 0 & 0 & 0 & 0 & 0 & 0 & 0 & 0 & 0 & L \end{bmatrix}. \tag{A.4}$$

APPENDIX B

New form of Equilibrium Equation of 2D Frame

The next equilibrium equation of the 2D frame was used in this study:

$$\mathbf{KD} = \mathbf{T}_a \mathbf{A} + \mathbf{T}_{bz} \mathbf{I}_z, \tag{B.1}$$

The matrices, which set up the last relation, are defined as below:

$$\mathbf{T}_a = [\mathbf{L}_1 \mathbf{K}_{a_1} \mathbf{L}_1^T \mathbf{D} \cdots \mathbf{L}_i \mathbf{K}_{a_i} \mathbf{L}_i^T \mathbf{D} \cdots \mathbf{L}_{nel} \mathbf{K}_{a_{nel}} \mathbf{L}_{nel}^T \mathbf{D}], \tag{B.2}$$

$$\mathbf{T}_{bz} = [\mathbf{L}_1 \mathbf{K}_{bz_1} \mathbf{L}_1^T \mathbf{D} \cdots \mathbf{L}_i \mathbf{K}_{bz_i} \mathbf{L}_i^T \mathbf{D} \cdots \mathbf{L}_{nel} \mathbf{K}_{bz_{nel}} \mathbf{L}_{nel}^T \mathbf{D}]. \tag{B.3}$$

In addition, the subsequent vectors include the members' cross-sectional properties:

$$\mathbf{A} = \{A_1 \ A_2 \ \cdots \ A_{nel}\}, \tag{B.4}$$

$$\mathbf{I}_z = \{I_{z_1} \ I_{z_2} \ \cdots \ I_{z_{nel}}\}^T. \tag{B.5}$$

APPENDIX C

Sherman–Morrison–Woodbury Formulas

The presented formulas in this section are utilized to calculate the inversion of a sum of two matrices. It is worth mentioning that these formulas invert a sum of two matrices accurately. They are named Sherman–Morrison–Woodbury formulas. In this article, Eq. (C.5) was utilized.

$$[\mathbf{A} - \mathbf{UV}]^{-1} = \mathbf{A}^{-1} + \mathbf{A}^{-1}\mathbf{U}(\mathbf{I} - \mathbf{VA}^{-1}\mathbf{U})^{-1}\mathbf{VA}^{-1}. \tag{C.1}$$

In this relation, the **U** matrix has $n \times m$ entries. Furthermore, the **V** matrix is an $m \times n$ matrix. The **I** matrix is an $m \times m$ identity matrix, and the **A** matrix has $n \times n$ entries. The correctness of the last equality can be proven as below:

$$\begin{aligned}
&[\mathbf{A} - \mathbf{UV}]\,[\mathbf{A}^{-1} + \mathbf{A}^{-1}\mathbf{U}(\mathbf{I} - \mathbf{VA}^{-1}\mathbf{U})^{-1}\mathbf{VA}^{-1}] \\
&\quad = \mathbf{I} - \mathbf{UVA}^{-1} + (\mathbf{U} - \mathbf{UVA}^{-1}\mathbf{U})\,(\mathbf{I} - \mathbf{VA}^{-1}\mathbf{U})^{-1}\mathbf{VA}^{-1} \\
&\quad = \mathbf{I} - \mathbf{UVA}^{-1} + \mathbf{U}\,(\mathbf{I} - \mathbf{VA}^{-1}\mathbf{U})\,(\mathbf{I} - \mathbf{VA}^{-1}\mathbf{U})^{-1}\mathbf{VA}^{-1} = \mathbf{I}.
\end{aligned} \tag{C.2}$$

If the **U** matrix is a column vector and the **V** matrix is a row vector, the last equation will have the succeeding shape:

$$[\mathbf{A} - \mathbf{UV}]^{-1} = \mathbf{A}^{-1} + \alpha\mathbf{A}^{-1}\mathbf{UVA}^{-1}, \quad \alpha = \frac{1}{(1 - \mathbf{VA}^{-1}\mathbf{U})}. \tag{C.3}$$

The subsequent relations show the correctness of Eq. (C.3):

$$\begin{aligned}
[A - UV]\left[A^{-1} + \frac{A^{-1}UVA^{-1}}{(\mathbf{1} - VA^{-1}U)}\right] &= I - UVA^{-1} + \frac{UVA^{-1} - UVA^{-1}UVA^{-1}}{(\mathbf{1} - VA^{-1}U)} \\
&= I - UVA^{-1} + \frac{U(\mathbf{1} - VA^{-1}U)\,VA^{-1}}{(\mathbf{1} - VA^{-1}U)} = I.
\end{aligned} \tag{C.4}$$

Generalizing Eq. (C.1) leads to the coming result:

$$[\mathbf{A} + \mathbf{UH}^{-1}\mathbf{V}]^{-1} = \mathbf{A}^{-1} - \mathbf{A}^{-1}\mathbf{U}(\mathbf{H} + \mathbf{VA}^{-1}\mathbf{U}^{-1}\mathbf{VA}^{-1}. \tag{C.5}$$

In this formula, the **U** matrix has $n \times m$ entries, and the **V** matrix has m rows and n columns. Moreover, **H** is an $m \times m$ diagonal matrix. The correctness of the last equality can be proven by utilizing the subsequent relations:

$$(A + U\,H^{-1}\,V)[A^{-1} - A^{-1}U(H + V\,A^{-1}\,U\,)^{-1}V\,A^{-1}]$$

$$
\begin{aligned}
&= I + U H^{-1} V A^{-1} - U(H + V A^{-1} U)^{-1} V A^{-1} \\
&- U H^{-1} V A^{-1} U(H + V A^{-1} U)^{-1} V A^{-1} \\
&= I + U H^{-1} V A^{-1} - (U + U H^{-1} V A^{-1} U)(H + V A^{-1} U)^{-1} V A^{-1} \\
&= I + U H^{-1} V A^{-1} - U H^{-1}(H + V A^{-1} U)(H + V A^{-1} U)^{-1} V A^{-1} \\
&= I + U H^{-1} V A^{-1} - U H^{-1} V A^{-1} = I. \qquad \text{(C.6)}
\end{aligned}
$$

As it was mentioned so far, Eq. (C.5) was utilized in this article.

APPENDIX D

The Steps of the Solution Procedure

1. Assuming that the geometry and topology of the structure are known, and the cross-sectional properties are calculated by employing the damage detection algorithms.
2. A simple load case is selected.
3. By utilizing the tactic presented in the second section, damaged elements of the structures are identified; therefore, the number of unknown parameters is reduced.
4. At this stage, the optimization procedure begins. It should be added that FORTRAN program was written by the authors to do the process.
5. The cross-sectional properties of the members are estimated.